Supporting Information

Probing the Dynamics of a His73-heme Alkaline Transition in a Destabilized Variant of Yeast Iso-1-Cytochrome *c* with Conformationally Gated Electron Transfer Methods

Swati Bandi and Bruce E. Bowler*

Department of Chemistry and Biochemistry and Center for Biomolecular Structure and Dynamics

The University of Montana, Missoula, Montana 59812

A. pH titrations as a function of gdnHCl concentration

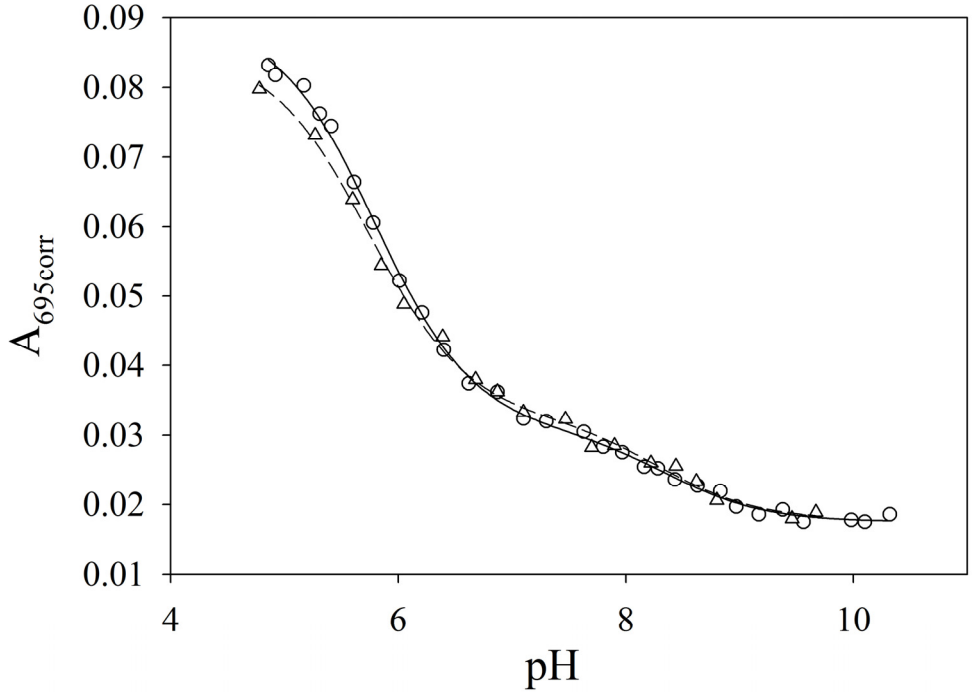

Figure S1. Plot of $A_{695corr}$ versus pH for AcH73 iso-1-cytochrome *c* at room temperature (22 ± 1 ºC) in 0.1 M NaCl in the presence of 0.2 M gdnHCl showing forward (○) and backward (Δ) titration curves. The solid curves are fits to eq 1 as described in the Experimental Section.

Table S1. Thermodynamic parameters from pH titration in 0.1 M NaCl at 22 ± 1 ºC for the AcH73 variant of iso-1-cytochrome *c*.[a]

[gdnHCl] (M)	pK_{C1}	pK_{H1}	pK_{C2}
0.1 (Forward)	-0.44 ± 0.08	6.29 ± 0.17	-2.92 ± 0.50
0.1 (Backward)	-0.66 ± 0.18	6.21 ± 0.31	-3.04 ± 0.43
0.2 (Forward)	-0.74 ± 0.20	6.28 ± 0.24	-3.33 ±0.24
0.2 (Backward)	-0.91 ± 0.08	6.19 ± 0.26	-3.51 ± 0.27
0.3 (Forward)	-0.84 ± 0.07	6.37 ± 0.18	-3.32 ± 0.09
0.3 (Backward)	-0.99 ± 0.22	6.11 ± 0.16	-3.63 ± 0.24

[a] Parameters are the average and standard deviation from three trials for fits to eq 1 in the Experimental Section.

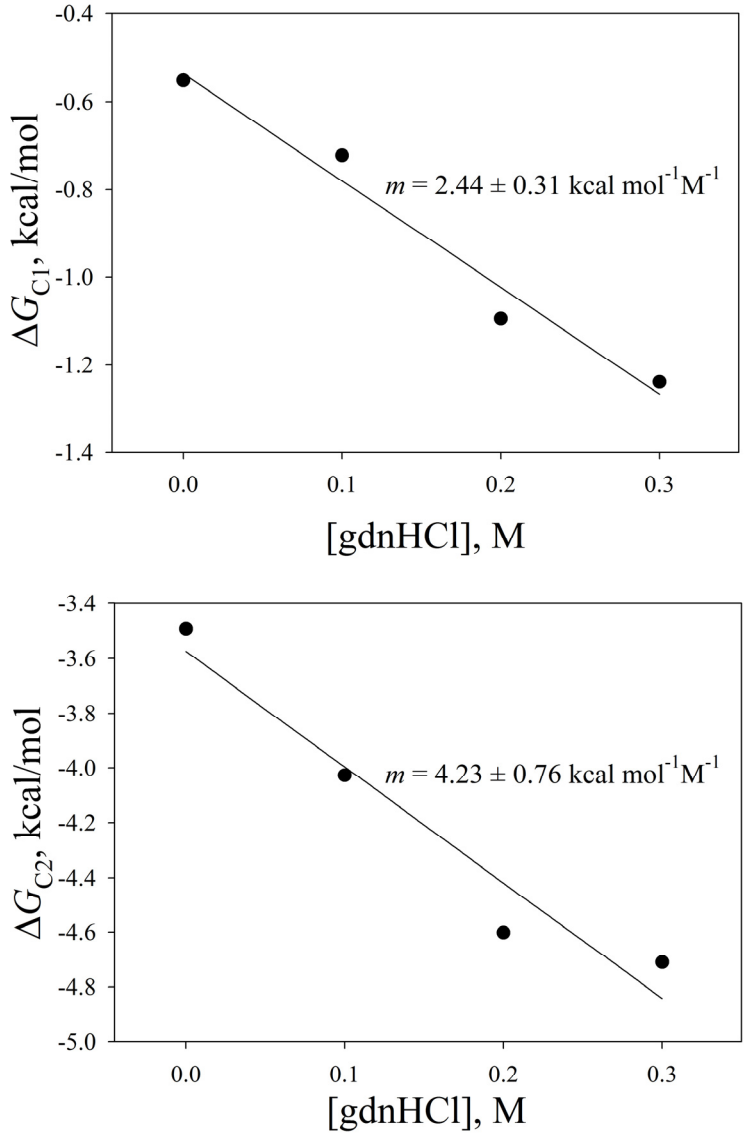

Figure S2. Plots of Free Energy verses gdnHCl concentration for the AcH73 variant of iso-1 Cyt *c*. The free energies, ΔG_{C1} and ΔG_{C2}, represent formation of the His73-heme and Lys79-heme alkaline conformers, respectively. ΔG values were calculated as $\Delta G = 2.303RTpK$ where pK_{C1} and pK_{C2} are used for the pK values. The data in Figure 3 of the main text were also fit using $pK_{a,2}$ values of 9.4 and 11.1 (values obtained from pH jump data in the main text), instead of the standard constraint of 10.8. No significant changes were observed for the $pK_{a,1}$ of His, pK_{C1} or the m-value derived from the slopes of plots of ΔG versus gdnHCl concentration (with $pK_{a,2}$ = 11.1, m-values obtained are 2.4 ± 0.3 and 4.5 ± 0.8; with $pK_{a,2}$ as 9.4, m-values obtained are 3.2 ± 0.9 and 5.3 ± 1.3) when the alternate values of $pK_{a,2}$ were used. Thus, the choice of $pK_{a,2}$ has minimal effect on the thermodynamic parameters obtained from these data.

B. pH jump Stopped-flow Data for the AcH73 Variant in 0.1 M NaCl and at 25 °C

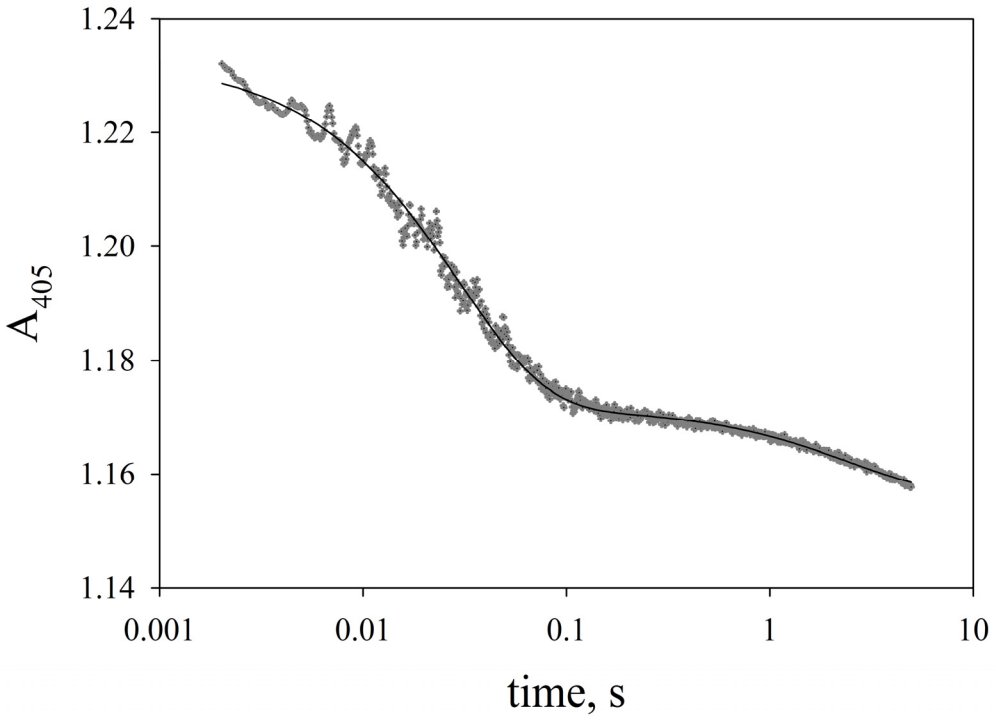

Figure S3. Plot of absorbance at 405 nm, A_{405}, as a function of time from 5 s downward pH jump data collected at 25º C and pH 5 for the AcH73 variant of iso-1-Cyt*c*. The starting pH was 7.8 (0.1 M NaCl). The buffer used to produce the final pH was 10 mM acetate, pH 5 in the presence of 0.1 M NaCl. The time scale is logarithmic. The solid curve is a fit of the data to the equation for a two exponential decay.

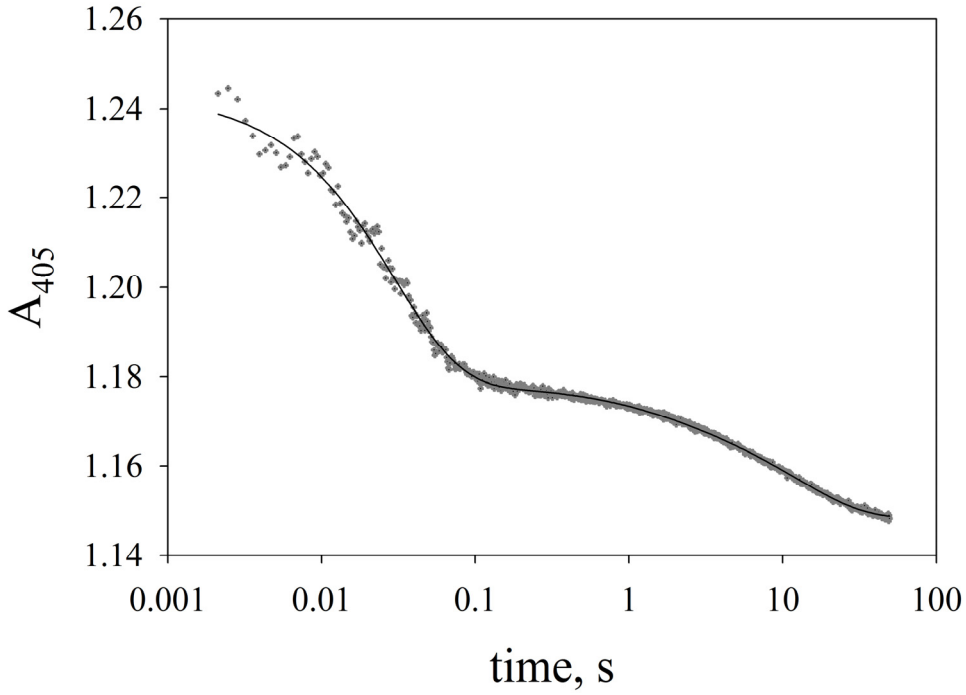

Figure S4. Plot of absorbance at 405 nm, A_{405}, as a function of time from 50 s downward pH jump data collected at 25º C and pH 5 for the AcH73 variant of iso-1-Cyt*c*. The starting pH was 7.8 (0.1 M NaCl). The buffer used to produce the final pH was 10 mM acetate, pH 5 in the presence of 0.1 M NaCl. The time scale is logarithmic. The solid curve is a fit of the data to a two exponential decay equation.

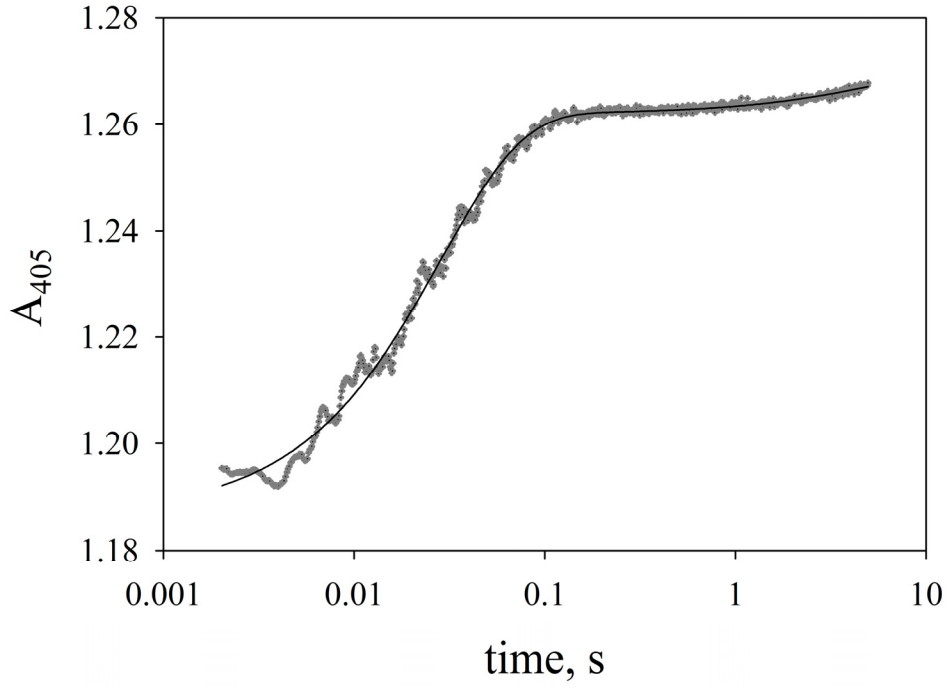

Figure S5. Plot of absorbance at 405 nm, A_{405}, as a function of time from 5 s upward pH jump data collected at 25º C and pH 7.2 for the AcH73 variant of iso-1-Cyt*c*. The starting pH was 5.0 (0.1 M NaCl). The buffer used to produce the final pH was 10 mM NaH_2PO_4, pH 7.2 in the presence of 0.1 M NaCl. The time scale is logarithmic. The solid curve is a fit of the data to a two exponential rise to maximum equation.

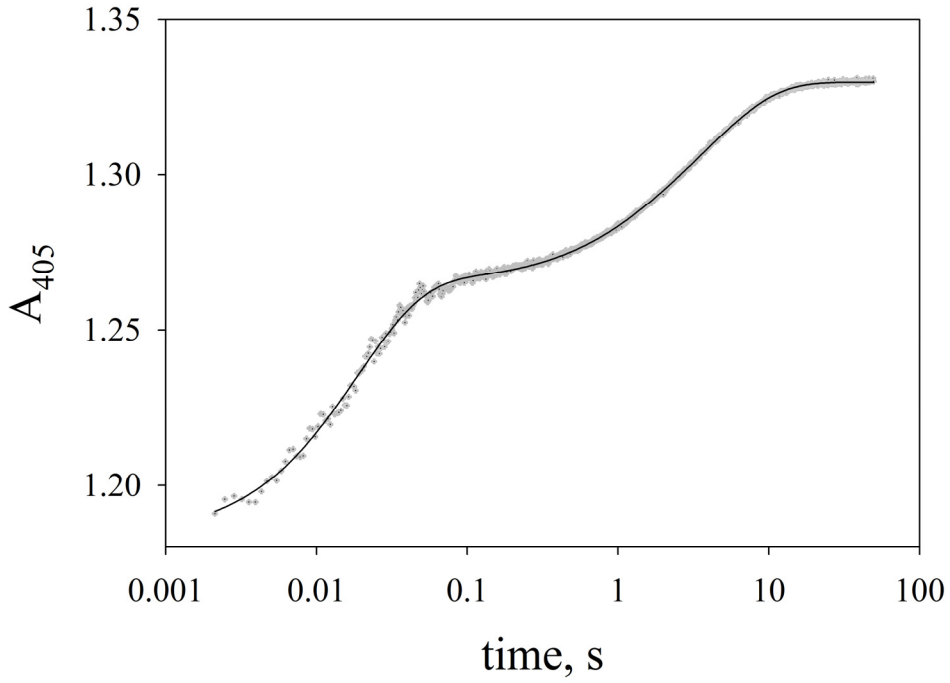

Figure S6. Plot of absorbance at 405 nm, A_{405}, as a function of time from 50s upward pH jump data collected at 25º C and pH 9 for the AcH73 variant of iso-1-Cyt*c*. The starting pH was 5.0 (0.1 M NaCl). The buffer used to produce the final pH was 10 mM H_3BO_3, pH 9 in the presence of 0.1 M NaCl. The time scale is logarithmic. The solid curve is a fit of the data to a two exponential rise to maximum equation.

Table S2. k_{obs} data for fast kinetic phase from upward pH jumps experiments.[a,b]

pH	k_{obs}, s^{-1}	pH	k_{obs}, s^{-1}	pH	k_{obs}, s^{-1}
5.8	36.9 ± 0.8	7.8	32.5 ± 1.0	9.8	46.3 ± 3.6
6.0	39.4 ± 2.2	8.0	33.4 ± 0.7	10.0	47.7 ± 2.8
6.2	39.0 ± 0.8	8.2	37.0 ± 1.1	10.2	49.7 ± 3.2
6.4	38.2 ± 0.7	8.4	36.1 ± 1.8	10.4	52.4 ± 5.2
6.6	37.8 ± 2.1	8.6	36.6 ± 1.5	10.6	44.4 ± 4.8
6.8	39.4 ± 0.9	8.8	39.3 ± 1.6	10.8	37.8 ± 8.9
7.0	33.6 ± 1.6	9.0	41.7 ± 2.9	11.0	22.1 ± 7.2
7.2	35.8 ± 0.8	9.2	42.8 ± 3.7	11.2	20.0 ± 0.2
7.4	34.4 ± 1.1	9.4	44.9 ± 3.3		
7.6	34.6 ± 1.1	9.6	47.6 ± 4.1		

[a] Data from pH 5.8 to 11.2 are the average of three data sets, two with data collected on a 5 s time scale and one with data collected on a 50 s timescale. Each data set was composed of at least 5 kinetic traces at each pH.

[b] Data collected on a 5 s time scale were fit to a single exponential equation and a double exponential equation at each pH. Data collected on a 50 second time were fit to a double exponential equation at each pH.

Table S3. k_{obs} data for slow kinetic phase from upward pH jump experiments. [a,b]

pH	k_{obs}, s^{-1}	pH	k_{obs}, s^{-1}	pH	k_{obs}, s^{-1}
5.8	0.045 ± 0.008	7.8	0.119 ± 0.001	9.8	0.76 ± 0.01
6.0	0.084 ± 0.008	8.0	0.124 ± 0.002	10.0	0.98 ± 0.02
6.2	0.085 ± 0.007	8.2	0.139 ± 0.008	10.2	1.31 ± 0.02
6.4	0.099 ± 0.009	8.4	0.157 ± 0.001	10.4	2.130 ± 0.003
6.6	0.106 ± 0.004	8.6	0.182 ± 0.002	10.6	3.0 ± 0.1
6.8	0.102 ± 0.01	8.8	0.214 ± 0.001	10.8	4.5 ± 0.4
7.0	0.101 ± 0.003	9.0	0.287 ± 0.001	11.0	5 ± 3
7.2	0.096 ± 0.002	9.2	0.350 ± 0.008	11.2	0.205 ± 0.048
7.4	0.098 ± 0.002	9.4	0.450 ± 0.006		
7.6	0.107 ± 0.004	9.6	0.586 ± 0.007		

[a] These values are the average and standard deviation from a single 50 s data set of pH jump experiments. Each data set was composed of at least 5 kinetic traces at each pH.

[b] The data were fit to a double exponential equation at each pH to extract the k_{obs} for the slow phase.

Table S4. Amplitude data for fast kinetic phase from upward pH jumps. [a,b]

pH	Amplitude (absorbance units)	pH	Amplitude (absorbance units)	pH	Amplitude (absorbance units)
5.8	0.029 ± 0.006	7.8	0.084 ± 0.004	9.8	0.086 ± 0.003
6.0	0.041 ± 0.001	8.0	0.083 ± 0.001	10.0	0.084 ± 0.003
6.2	0.047 ± 0.0004	8.2	0.083 ± 0.004	10.2	0.080 ± 0.003
6.4	0.043 ± 0.003	8.4	0.088 ± 0.004	10.4	0.073 ± 0.005
6.6	0.055 ± 0.005	8.6	0.086 ± 0.001	10.6	0.064 ± 0.009
6.8	0.055 ± 0.003	8.8	0.089 ± 0.002	10.8	0.061 ± 0.014
7.0	0.074 ± 0.004	9.0	0.088 ± 0.002	11.0	0.081 ± 0.018
7.2	0.071 ± 0.005	9.2	0.090 ± 0.004	11.2	0.105 ± 0.001
7.4	0.075 ± 0.001	9.4	0.093 ± 0.001		
7.6	0.074 ± 0.006	9.6	0.089 ± 0.004		

[a] Data from pH 5.8 to 11.2 are the average of three data sets, two with data collected on a 5 s time scale and one with data collected on a 50 s timescale. Each data set was composed of at least 5 kinetic traces at each pH.

[b] Data collected on a 5 s time scale were fit to a single exponential equation and a double exponential equation at each pH. Data collected on a 50 second time were fit to a double exponential equation at each pH.

Table S5. Amplitude data for slow kinetic phase from upward pH jump experiments.[a,b]

pH	Amplitude (absorbance units)	pH	Amplitude (absorbance units)	pH	Amplitude (absorbance units)
5.8	0.0047 ± 0.0005	7.8	0.0195 ± 0.0003	9.8	0.0744 ± 0.0005
6.0	0.0064 ± 0.0002	8.0	0.0248 ± 0.0002	10.0	0.0741 ± 0.0004
6.2	0.0076 ± 0.0003	8.2	0.0305 ± 0.0002	10.2	0.0722 ± 0.0007
6.4	0.0073 ± 0.0003	8.4	0.0391 ± 0.0007	10.4	0.0695 ± 0.001
6.6	0.0075 ± 0.0007	8.6	0.0461 ± 0.0005	10.6	0.0664 ± 0.001
6.8	0.0086 ± 0.0008	8.8	0.0526 ± 0.0002	10.8	0.0602 ± 0.007
7.0	0.0114 ± 0.0003	9.0	0.0620 ± 0.0002	11.0	0.0340 ± 0.025
7.2	0.0130 ± 0.0003	9.2	0.067 ± 0.001	11.2	0.0038 ± 0.0006
7.4	0.0147 ± 0.0003	9.4	0.0707 ± 0.0005		
7.6	0.0171 ± 0.0001	9.6	0.0729 ± 0.0007		

[a] These values are the average and standard deviation from a single data 50 s set of pH jump experiments. Each data set was composed of at least 5 kinetic traces at each pH.

[b] The data were fit to a double exponential equation at each pH to extract the k_{obs} for the slow phase.

Table S6. k_{obs} and amplitude data for fast kinetic phase from downward pH jump experiments.[a,b]

pH	k_{obs}, s^{-1}	Amplitude (absorbance units)
5.0	33.0 ± 1.5	0.067 ± 0.009
5.2	35.1 ± 1.1	0.060 ± 0.001
5.4	35.6 ± 0.3	0.056 ± 0.001
5.6	35.3 ± 1.6	0.051 ± 0.001
5.8	35.4 ± 4.3	0.040 ± 0.002
6.0	33.9 ± 1.3	0.035 ± 0.005
6.2	36.0 ± 1.6	0.027 ± 0.001
6.4	35.0 ± 1.0	0.019 ± 0.001

[a] Data are the average of three data sets, two with data collected on a 5 s time scale and one with data collected on a 50 s timescale. Each data set was composed of at least 5 kinetic traces at each pH.

[b] Data collected on a 5 s time scale were fit to a single exponential equation and a double exponential equation at each pH. Data collected on a 50 second time were fit to a double exponential equation at each pH.

Table S7. k_{obs} and amplitude data for slow kinetic phase from downward pH jump experiments.[a,b]

pH	k_{obs}, s^{-1}	Amplitude (absorbance units)
5.0	0.113 ± 0.002	0.0270 ± 0.0004
5.2	0.115 ± 0.001	0.0260 ± 0.0003
5.4	0.112 ± 0.001	0.0240 ± 0.0006
5.6	0.115 ± 0.002	0.0210 ± 0.0003
5.8	0.116 ± 0.003	0.0180 ± 0.0005
6.0	0.107 ± 0.013	0.0130 ± 0.0007
6.2	0.106 ± 0.015	0.0110 ± 0.0003
6.4	0.103 ± 0.021	0.0007 ± 0.0007

[a] These values are the average and standard deviation from a single 50 s data set of pH jump experiments. Each data set was composed of at least 5 kinetic traces at each pH.

[b] The data were fit to a double exponential equation at each pH to extract the k_{obs} for the slow phase.

C. Gated Electron Transfer Kinetic Data.

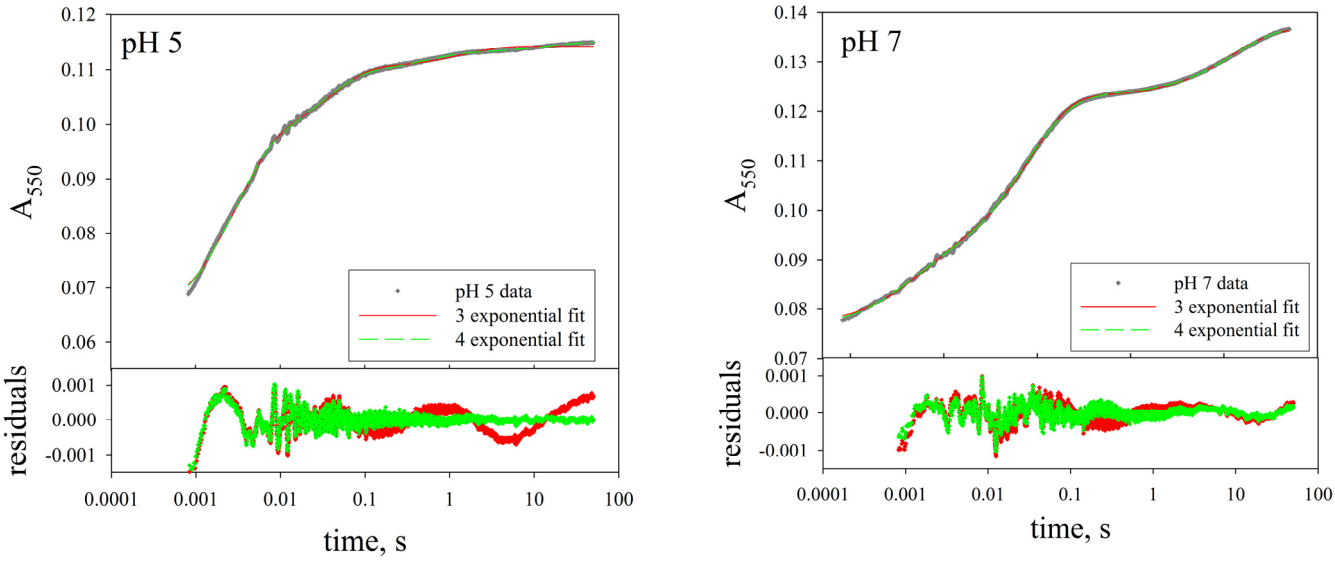

Figure S7. Plots of absorbance at 550 nm as a function of time (top panels) and residuals (bottom panels) for 3 and 4 exponential rise to maximum fits to the data as a function of time for ~5 mM a_6Ru^{2+} at pH 5 (left, 10 mM acetic acid buffer) and pH 7 (right, 10 mM NaH_2PO_4 buffer) in 0.1 M NaCl.

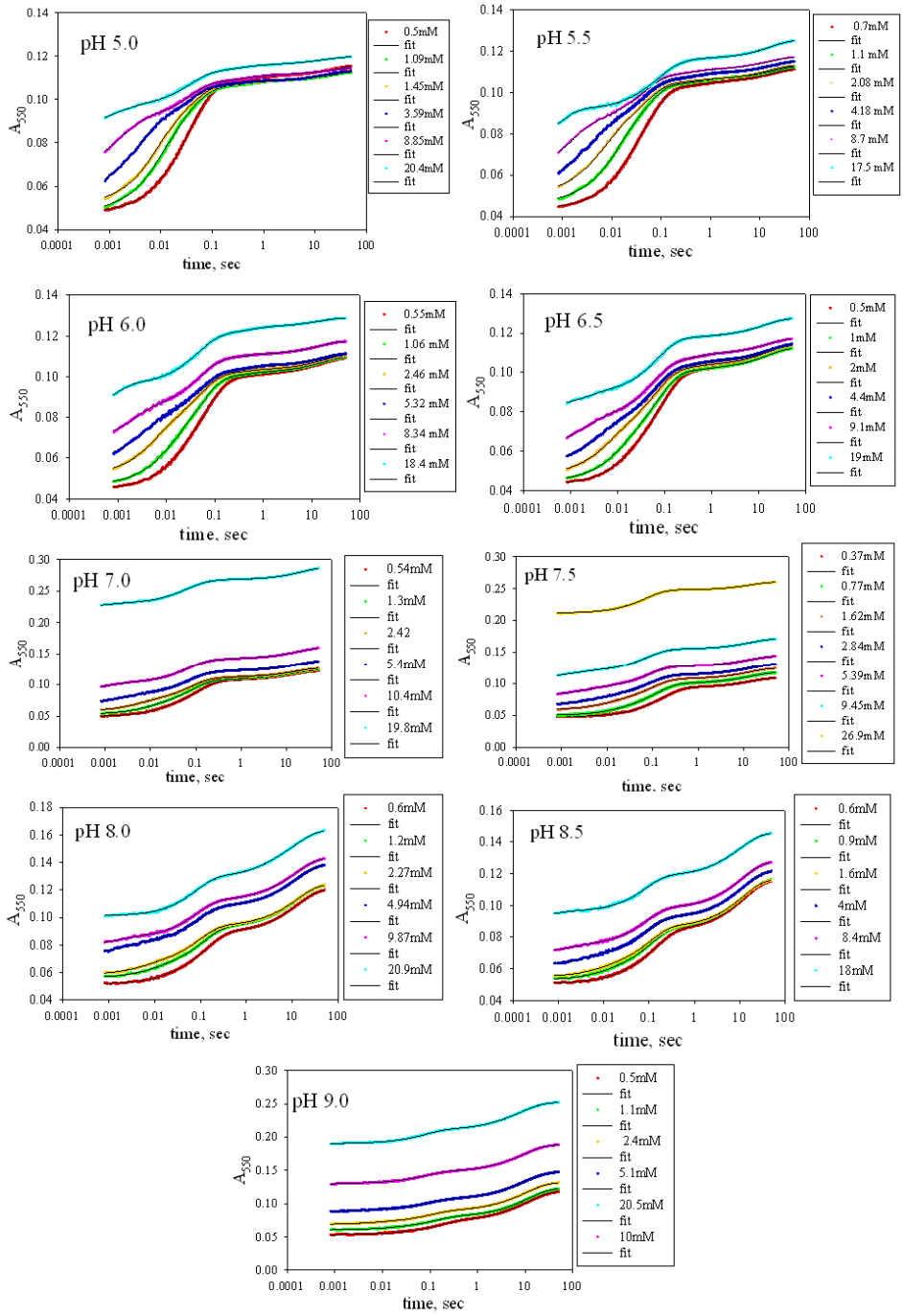

Figure S8. Plots of absorbance at 550 nm as a function of time at different concentrations of a_6Ru^{2+} at pH 5.0, 5.5, 6.0, 6.5, 7.0, 7.5, 8.0, 8.5 and 9.0. Buffers are all 10 mM containing 0.1 M NaCl. All data were collected at 25 ºC. The solid lines are fits to a four exponential rise to maximum equation. Rate constant and amplitude parameters from these fits are collected in Tables S8 to S11.

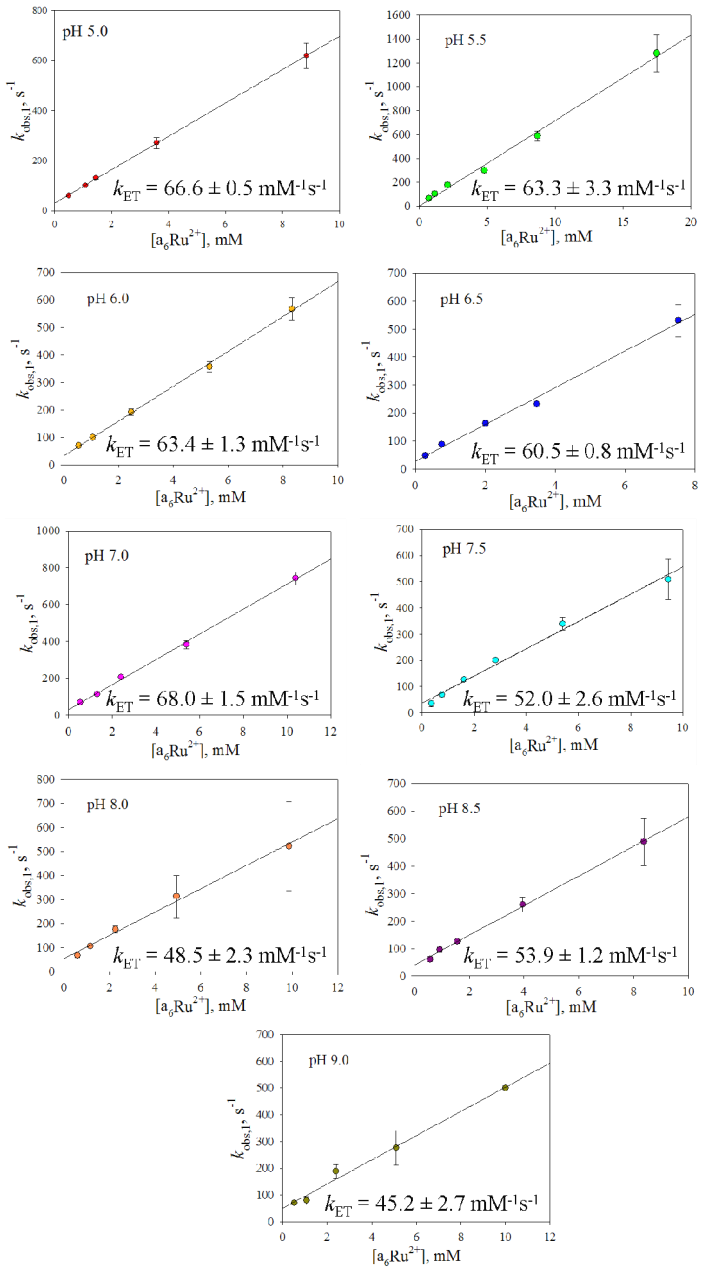

Figure S9. Plots of observed rate constant, $k_{obs,1}$, for the reaction of a_6Ru^{2+} with the native conformer of the AcH73 variant (fastest phase) at 25 ºC as a function of a_6Ru^{2+} concentration for pH 5, 5.5, 6, 6.5, 7, 7.5, 8, 8.5 and 9. Buffers, as described in main text, are 10 mM and contain 0.1 M NaCl. The solid lines are fits to a linear equation. The rate constants shown in this figure are collected in Table S8. Values for the highest concentration, i.e., ~20 mM for fast phase, are mostly not included in these plots due to the relatively large errors in k_{obs} at this concentration of a_6Ru^{2+} (see Table S8) and thus were not used in evaluating k_{ET}. At 20 mM a_6Ru^{2+} most of the fast phase amplitude occurs in the mixing dead time, as can be seen in Figure S8.

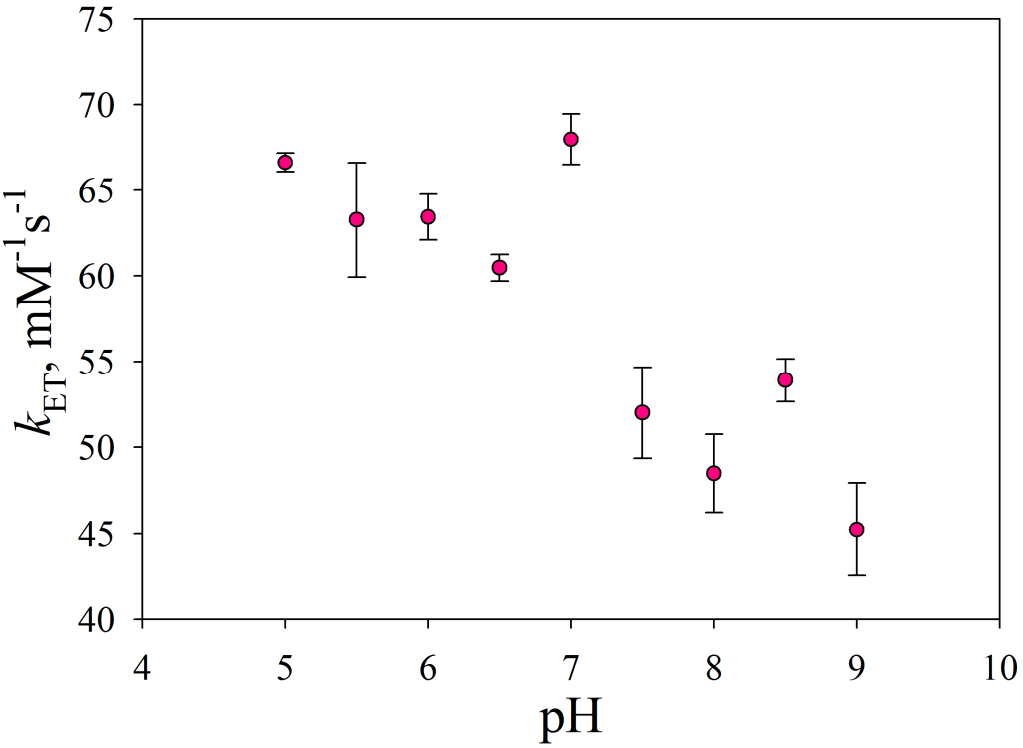

Figure S10. Plot of k_{ET} ($mM^{-1}s^{-1}$) as a function of pH at 25 ^{o}C. The values for k_{ET} are obtained from fits to eq 5 in the main text as shown in Figure S9.

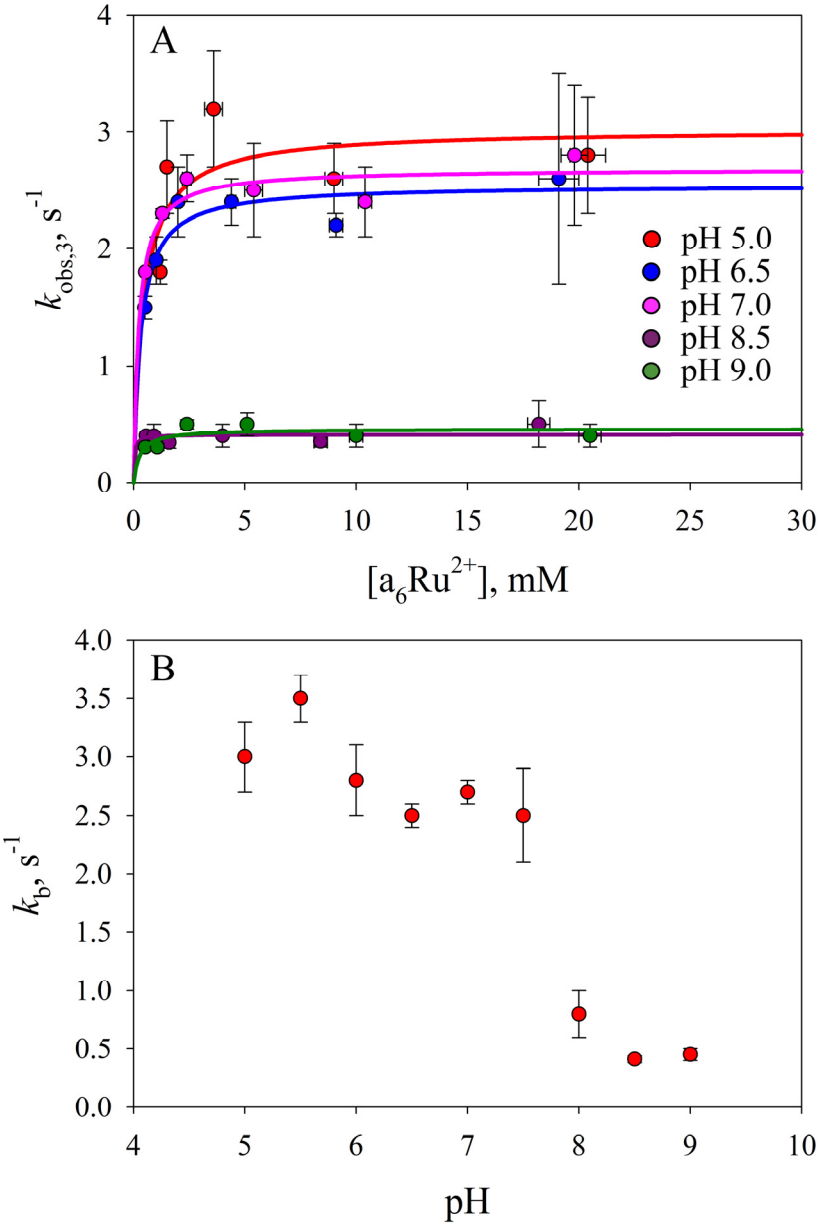

Figure S11. (A) Plots of $k_{obs,3}$ versus the concentration of a_6Ru^{2+} for the reaction of a_6Ru^{2+} with the AcH73 variant at selected pH values between pH 5 and 9 in 10 mM buffers containing 0.1 M NaCl at 25 ºC. The solid lines are fits to eq 6 (main text) which gives values for k_b and k_f as defined in Figure 6 (main text). k_b and k_f from these fits are collected in Table S13. (B) Plot of k_b versus pH. k_b is derived from fits of eq 6 in the main text to $k_{obs,3}$ versus a_6Ru^{2+} concentration data. k_b values are from Table S13.

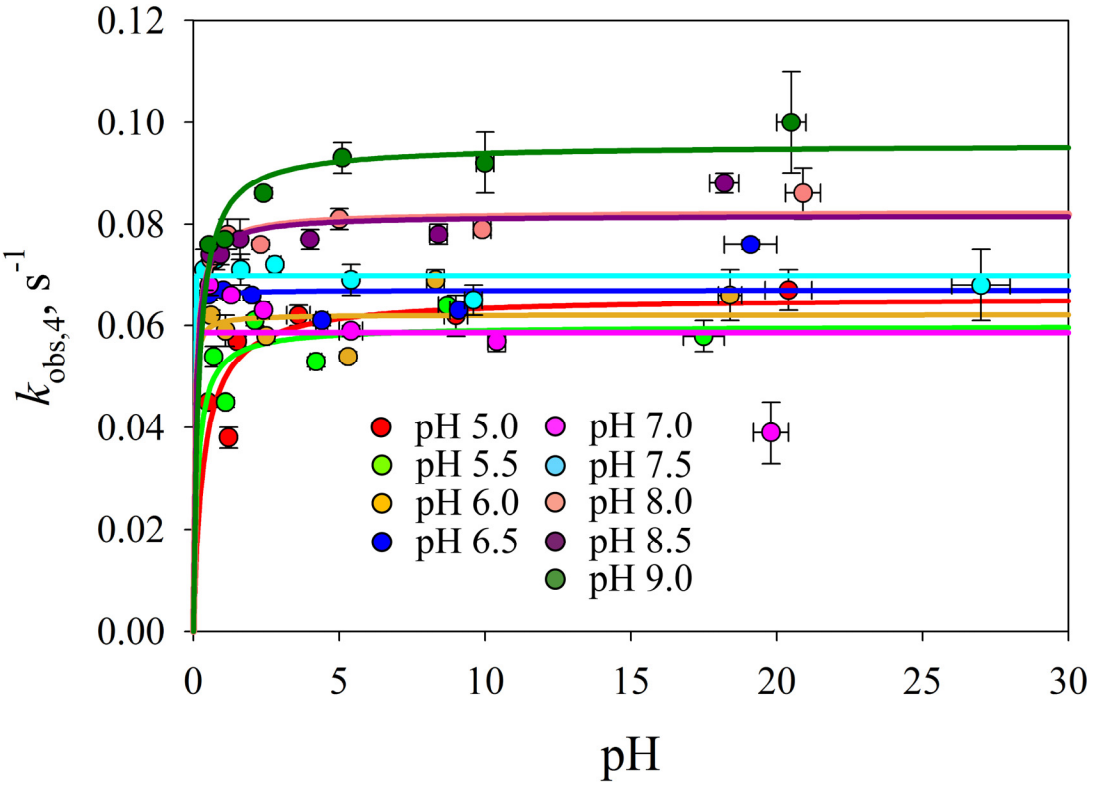

Figure S12. Plots of $k_{obs,4}$ versus the concentration of a_6Ru^{2+} for the reaction of a_6Ru^{2+} with the AcH73 variant from pH 5 to 9 in 10 mM buffers containing 0.1 M NaCl at 25 ºC. The solid lines are fits to eq 6 (main text) which gives values for k_b and k_f as defined in Figure 6 (main text). k_b and k_f from these fits are collected in Table S14.

Table S8. Fast rate constant, $k_{obs,1}$, and its amplitude for the reduction of AcH73 iso-1-cytochrome *c* by a_6Ru^{2+} as a function of pH and [a_6Ru^{2+}] from four exponential fits to the data in Figure S8.

pH	[a_6Ru^{2+}], mM	k_{obs}, s^{-1}	Amplitude
5.0	0.5 ± 0.1	60 ± 3	0.015 ± 0.002
	1.1 ± 0.1	102 ± 2	0.030 ± 0.001
	1.5 ± 0.1	132 ± 5	0.0312 ± 0.0010
	3.6 ± 0.4	271 ± 22	0.0286 ± 0.0004
	9.0 ± 0.4	619 ± 50	0.0225 ± 0.0010
	20.4 ± 0.8	1215 ± 346	0.0148 ± 0.0050
5.5	0.7 ± 0.1	63.4 ± 4	0.0130 ± 0.0008
	1.1 ± 0.1	102 ± 2	0.0233 ± 0.0007
	2.1 ± 0.1	175 ± 3	0.0262 ± 0.0002
	4.2 ± 0.2	298 ± 11	0.0251 ± 0.0006
	8.7 ± 0.3	587 ± 42	0.0221 ± 0.0010
	17.5 ± 0.7	1280 ± 152	0.0182 ± 0.0030
6.0	0.6 ± 0.1	69 ± 4	0.0107 ± 0.0007
	1.1 ± 0.1	99 ± 7	0.0174 ± 0.0009
	2.5 ± 0.1	192 ± 12	0.0235 ± 0.0040
	5.3 ± 0.1	357 ± 20	0.0195 ± 0.0003
	8.3 ± 0.3	568 ± 41	0.0177 ± 0.0010
	18.4 ± 0.4	1284 ± 390	0.0154 ± 0.0080
6.5	0.52 ± 0.02	69 ± 2	0.0114 ± 0.0003
	1.02 ± 0.03	99 ± 2	0.0162 ± 0.0002
	2.0 ± 0.1	168 ± 6	0.0188 ± 0.0003
	4.4 ± 0.2	299 ± 12	0.0181 ± 0.0005
	9.1 ± 0.3	592 ± 52	0.0155 ± 0.0010
	19.1 ± 0.9	1037 ± 273	0.0107 ± 0.0030
7.0	0.54 ± 0.02	69 ± 6	0.0087 ± 0.0002
	1.30 ± 0.04	113 ± 3	0.0127 ± 0.0002
	2.4 ± 0.2	206 ± 9	0.0145 ± 0.0004
	5.4 ± 0.4	382 ± 24	0.0132 ± 0.0004
	10.4 ± 0.3	742 ± 35	0.0123 ± 0.0010
	19.8 ± 0.6	1497 ± 428	0.0101 ± 0.0050
7.5	0.37 ± 0.04	34 ± 11	0.0038 ± 0.0008
	0.77 ± 0.06	68 ± 8	0.0069 ± 0.0008
	1.62 ± 0.04	125 ± 8	0.0161 ± 0.0100
	2.8 ± 0.2	201 ± 3	0.0116 ± 0.0002
	5.4 ± 0.1	339 ± 25	0.0119 ± 0.0003
	9.4 ± 0.3	509 ± 77	0.0100 ± 0.0007
	27 ± 1	1765 ± 137	0.0058 ± 0.0010

8.0	0.61 ± 0.04	67 ± 9	0.0040 ± 0.0002
	1.17 ± 0.03	106 ± 5	0.006 ± 0.001
	2.3 ± 0.1	175 ± 14	0.007 ± 0.001
	4.9 ± 0.1	312 ± 88	0.007 ± 0.001
	9.9 ± 0.3	521 ± 184	0.006 ± 0.001
	20.9 ± 0.6	1175 ± 480	0.002 ± 0.002
8.5	0.57 ± 0.03	61 ± 5	0.0037 ± 0.0002
	0.92 ± 0.11	96 ± 10	0.0052 ± 0.0002
	1.6 ± 0.1	126 ± 8	0.0057 ± 0.0004
	4.0 ± 0.1	259 ± 27	0.0058 ± 0.0002
	8.4 ± 0.3	489 ± 86	0.005 ± 0.001
	18.2 ± 0.5	1555 ± 127[a]	0.007 ± 0.010 [a]
9.0	0.53 ± 0.03	71 ± 13	0.0020 ± 0.0002
	1.07 ± 0.03	80 ± 13	0.0029 ± 0.0001
	2.4 ± 0.1	189 ± 26	0.0033 ± 0.0001
	5.1 ± 0.1	277 ± 64	0.0031 ± 0.0003
	10.0 ± 0.3	500 ± 6	0.003 ± 0.002
	20.5 ± 0.5	1511 ± 555[a]	0.0012 ± 0.0007 [a]

[a] This rate constant value is taken from one trial as values from the other trials showed variation due to the low observable amplitude at the highest concentration of a_6Ru^{2+}.

Table S9. First intermediate rate constant, $k_{obs,2}$, and its amplitude for the reduction of AcH73 iso-1-cytochrome *c* by a_6Ru^{2+} as a function of pH and $[a_6Ru^{2+}]$ at 25 °C from four exponential fits to the data in Figure S8.

pH	$[a_6Ru^{2+}]$, mM	k_{obs}, s^{-1}	Amplitude
5.0	0.5 ± 0.1	21.0 ± 0.3	0.0456 ± 0.0020
	1.2 ± 0.1	26 ± 1	0.0265 ± 0.0010
	1.5 ± 0.1	26 ± 1	0.0234 ± 0.0010
	3.6 ± 0.4	28 ± 2	0.0193 ± 0.0010
	9.0 ± 0.4	31 ± 1	0.0173 ± 0.0004
	20.4 ± 0.8	27 ± 1	0.0166 ± 0.0004
5.5	0.7 ± 0.1	18 ± 0.2	0.0454 ± 0.0009
	1.1 ± 0.1	23.0 ± 0.5	0.0333 ± 0.0008
	2.1 ± 0.1	23.0 ± 0.5	0.0268 ± 0.0003
	4.2 ± 0.2	25.4 ± 0.2	0.0237 ± 0.0006
	8.7 ± 0.3	24 ± 1	0.0227 ± 0.0004
	17.5 ± 0.7	12 ± 1	0.0199 ± 0.0014
6.0	0.6 ± 0.1	15 ± 0.4	0.0431 ± 0.0006
	1.1 ± 0.1	19 ± 1	0.0348 ± 0.0010
	2.5 ± 0.1	21 ± 1	0.0277 ± 0.0007
	5.3 ± 0.1	22.0 ± 0.4	0.0245 ± 0.0005
	8.3 ± 0.3	21 ± 1	0.0243 ± 0.0006
	18.4 ± 0.4	22.0 ± 0.3	0.0234 ± 0.0005
6.5	0.52 ± 0.02	12.0 ± 0.1	0.0444 ± 0.0010
	1.02 ± 0.03	14.0 ± 0.2	0.0386 ± 0.0005
	2.0 ± 0.1	16.0 ± 0.4	0.0333 ± 0.0002
	4.4 ± 0.2	17.4 ± 0.1	0.0302 ± 0.0006
	9.1 ± 0.3	18.2 ± 0.2	0.0288 ± 0.0004
	19.1 ± 0.9	15.0 ± 0.4	0.0286 ± 0.0005
7.0	0.54 ± 0.02	9.5 ± 0.1	0.0467 ± 0.0009
	1.30 ± 0.04	12.1 ± 0.1	0.0412 ± 0.0003
	2.4 ± 0.2	14.0 ± 0.3	0.0368 ± 0.0004
	5.4 ± 0.4	14.5 ± 0.3	0.0354 ± 0.0007
	10.4 ± 0.3	15 ± 1	0.0356 ± 0.0010
	19.8 ± 0.6	15.0 ± 1.3	0.0378 ± 0.0020
7.5	0.37 ± 0.04	5.6 ± 0.4	0.0420 ± 0.0050
	0.77 ± 0.06	8.6 ± 0.5	0.0410 ± 0.0010
	1.62 ± 0.04	11.0± 0.4	0.0375 ± 0.0003
	2.8 ± 0.2	12.0 ± 0.1	0.0352 ± 0.0003
	5.4 ± 0.1	13.0 ± 0.6	0.0341 ± 0.0010
	9.4 ± 0.3	13.1 ± 0.6	0.0337 ± 0.0010
	27 ± 1	14.1 ± 0.7	0.0343 ± 0.0020

8.0	0.61 ± 0.04	7.4 ± 0.1	0.0324 ± 0.0006
	1.17 ± 0.03	9.0 ± 0.3	0.0298 ± 0.0004
	2.3 ± 0.1	11.0 ± 0.6	0.0276 ± 0.0002
	4.9 ± 0.1	11.7 ± 0.5	0.0269 ± 0.0003
	9.9 ± 0.3	12.4 ± 0.6	0.0268 ± 0.0005
	20.9 ± 0.6	13.0 ± 0.5	0.0269 ± 0.0010
8.5	0.57 ± 0.03	7.0 ± 0.1	0.0294 ± 0.0003
	0.92 ± 0.11	9.9 ± 0.2	0.0269 ± 0.0005
	1.6 ± 0.1	10.0 ± 0.2	0.0255 ± 0.0002
	4.0 ± 0.1	11.0 ± 0.3	0.0241 ± 0.0003
	8.4 ± 0.3	12.0 ± 0.2	0.0233 ± 0.0003
	18.2 ± 0.5	12.0 ± 0.5	0.0215 ± 0.0005
9.0	0.53 ± 0.03	5.9 ± 0.1	0.0189 ± 0.0003
	1.07 ± 0.03	7.5 ± 0.1	0.0172 ± 0.0001
	2.4 ± 0.1	9.5 ± 0.2	0.0175 ± 0.0004
	5.1 ± 0.1	10.6 ± 0.4	0.0163 ± 0.0003
	10.0 ± 0.3	11.2 ± 1.2	0.0165 ± 0.0020
	20.5 ± 0.5	11.8 ± 0.3	0.0192 ± 0.0007

Table S10. Second intermediate rate constant, $k_{obs,3}$, and its amplitude for the reduction of AcH73 iso-1-cytochrome *c* by a_6Ru^{2+} as a function of pH and $[a_6Ru^{2+}]$ at 25 °C from four exponential fits to the data in Figure S8.

pH	$[a_6Ru^{2+}]$, mM	k_{obs}, s^{-1}	Amplitude
5.0	0.5 ± 0.1	1.5 ± 0.1	0.0027 ± 0.0001
	1.2 ± 0.1	1.8 ± 0.1	0.0032 ± 0.0001
	1.5 ± 0.1	2.7 ± 0.4	0.0020 ± 0.0002
	3.6 ± 0.4	3.2 ± 0.5	0.0022 ± 0.0003
	9.0 ± 0.4	2.6 ± 0.3	0.0040 ± 0.0003
	20.4 ± 0.8	2.8 ± 0.5	0.0029 ± 0.0006
5.5	0.7 ± 0.1	1.4 ± 0.1	0.0030 ± 0.0002
	1.1 ± 0.1	1.6 ± 0.1	0.0038 ± 0.0002
	2.1 ± 0.1	2.5 ± 0.2	0.0028 ± 0.0002
	4.2 ± 0.2	2.4 ± 0.05	0.0043 ± 0.0003
	8.7 ± 0.3	3.0 ± 0.3	0.0037 ± 0.0001
	17.5 ± 0.7	3.5 ± 0.8	0.0042 ± 0.0020
6.0	0.6 ± 0.1	2.0 ± 0.2	0.0026 ± 0.0003
	1.1 ± 0.1	2.1 ± 0.2	0.0029 ± 0.0003
	2.5 ± 0.1	2.8 ± 0.2	0.0029 ± 0.0003
	5.3 ± 0.1	2.6 ± 0.1	0.0039 ± 0.0001
	8.3 ± 0.3	3.4 ± 0.2	0.0027 ± 0.0004
	18.4 ± 0.4	2.2 ± 0.1	0.0044 ± 0.0002
6.5	0.52 ± 0.02	1.5 ± 0.1	0.0026 ± 0.0002
	1.02 ± 0.03	1.9 ± 0.2	0.0023 ± 0.0004
	2.0 ± 0.1	2.4 ± 0.3	0.0029 ± 0.0004
	4.4 ± 0.2	2.4 ± 0.2	0.0041 ± 0.0002
	9.1 ± 0.3	2.2 ± 0.1	0.0047 ± 0.0002
	19.1 ± 0.9	2.6 ± 0.9	0.0015 ± 0.0004
7.0	0.54 ± 0.02	1.8 ± 0.3	0.0031 ± 0.0004
	1.30 ± 0.04	2.3 ± 0.2	0.0036 ± 0.0002
	2.4 ± 0.2	2.6 ± 0.2	0.0039 ± 0.0004
	5.4 ± 0.4	2.5 ± 0.3	0.0037 ± 0.0004
	10.4 ± 0.3	2.4 ± 0.7	0.0034 ± 0.0010
	19.8 ± 0.6	2.8 ± 1.0	0.0016 ± 0.0002
7.5	0.37 ± 0.04	2.1 ± 1.5	0.0046 ± 0.0030
	0.77 ± 0.06	1.8 ± 1.3	0.0027 ± 0.0020
	1.62 ± 0.04	1.5 ± 1.1	0.0019 ± 0.0005
	2.8 ± 0.2	2.1 ± 0.3	0.0018 ± 0.0002
	5.4 ± 0.1	1.9 ± 1.4	0.0020 ± 0.0008
	9.4 ± 0.3	2.3 ± 2.6	0.0020 ± 0.0010
	27 ± 1	3.7 ± 1.5	0.0016 ± 0.0008

8.0	0.61 ± 0.04	0.46 ± 0.1	0.0025 ± 0.0003
	1.17 ± 0.03	0.74 ± 0.4	0.0024 ± 0.0001
	2.3 ± 0.1	1.3 ± 1.0	0.0026 ± 0.0003
	4.9 ± 0.1	0.7 ± 0.2	0.0025 ± 0.0004
	9.9 ± 0.3	0.6 ± 0.4	0.0039 ± 0.0007
	20.9 ± 0.6	0.6 ± 0.1	0.0066 ± 0.0005
8.5	0.57 ± 0.03	0.40 ± 0.02	0.0029 ± 0.0001
	0.92 ± 0.11	0.4 ± 0.1	0.0032 ± 0.0005
	1.6 ± 0.1	0.34 ± 0.05	0.0025 ± 0.0007
	4.0 ± 0.1	0.4 ± 0.1	0.0027 ± 0.0006
	8.4 ± 0.3	0.35 ± 0.05	0.0034 ± 0.0005
	18.2 ± 0.5	0.5 ± 0.2	0.0034 ± 0.0004
9.0	0.53 ± 0.03	0.30 ± 0.01	0.0066 ± 0.0003
	1.07 ± 0.03	0.30 ± 0.03	0.0057 ± 0.0010
	2.4 ± 0.1	0.50 ± 0.04	0.0054 ± 0.0004
	5.1 ± 0.1	0.5 ± 0.1	0.0055 ± 0.0007
	10.0 ± 0.3	0.4 ± 0.1	0.0069 ± 0.0030
	20.5 ± 0.5	0.4 ± 0.1	0.0098 ± 0.0020

Table S11. Slow rate constant, $k_{obs,4}$, and its amplitude for the reduction of AcH73 iso-1-cytochrome *c* by a_6Ru^{2+} as a function of pH and [a_6Ru^{2+}] at 25 °C from four exponential fits to the data in Figure S8.

pH	[a_6Ru^{2+}], mM	k_{obs}, s^{-1}	Amplitude
5.0	0.5 ± 0.1	0.045 ± 0.001	0.0054 ± 0.0001
	1.2 ± 0.1	0.038 ± 0.002	0.0050 ± 0.0001
	1.5 ± 0.1	0.057 ± 0.001	0.0053 ± 0.0001
	3.6 ± 0.4	0.062 ± 0.002	0.0052 ± 0.0003
	9.0 ± 0.4	0.062 ± 0.004	0.0036 ± 0.0002
	20.4 ± 0.8	0.067 ± 0.004	0.0043 ± 0.0005
5.5	0.7 ± 0.1	0.054 ± 0.002	0.0069 ± 0.0001
	1.1 ± 0.1	0.045 ± 0.001	0.0064 ± 0.0003
	2.1 ± 0.1	0.061 ± 0.001	0.0072 ± 0.0001
	4.2 ± 0.2	0.053 ± 0.001	0.0064 ± 0.0002
	8.7 ± 0.3	0.064 ± 0.001	0.0068 ± 0.0003
	17.5 ± 0.7	0.058 ± 0.003	0.0099 ± 0.0004
6.0	0.6 ± 0.1	0.062 ± 0.001	0.0082 ± 0.0001
	1.1 ± 0.1	0.059 ± 0.003	0.0079 ± 0.0001
	2.5 ± 0.1	0.058 ± 0.001	0.0076 ± 0.0001
	5.3 ± 0.1	0.054 ± 0.001	0.0067 ± 0.0001
	8.3 ± 0.3	0.069 ± 0.002	0.0070 ± 0.0002
	18.4 ± 0.4	0.066 ± 0.005	0.0053 ± 0.0005
6.5	0.52 ± 0.02	0.066 ± 0.001	0.0110 ± 0.0001
	1.02 ± 0.03	0.067 ± 0.001	0.0110 ± 0.0001
	2.0 ± 0.1	0.066 ± 0.001	0.0110 ± 0.0001
	4.4 ± 0.2	0.061 ± 0.001	0.0095 ± 0.0001
	9.1 ± 0.3	0.063 ± 0.001	0.0085 ± 0.0002
	19.1 ± 0.9	0.076 ± 0.001	0.0095 ± 0.0002
7.0	0.54 ± 0.02	0.068 ± 0.002	0.0145 ± 0.0001
	1.30 ± 0.04	0.066 ± 0.001	0.0145 ± 0.0001
	2.4 ± 0.2	0.0630 ± 0.0002	0.0148 ± 0.0002
	5.4 ± 0.4	0.059 ± 0.001	0.0156 ± 0.0002
	10.4 ± 0.3	0.057 ± 0.002	0.0182 ± 0.0003
	19.8 ± 0.6	0.039 ± 0.006	0.018 ± 0.003
7.5	0.37 ± 0.04	0.071 ± 0.004	0.0165 ± 0.0008
	0.77 ± 0.06	0.073 ± 0.002	0.0169 ± 0.0002
	1.62 ± 0.04	0.071 ± 0.003	0.0167 ± 0.0003
	2.8 ± 0.2	0.072 ± 0.001	0.0166 ± 0.0007
	5.4 ± 0.1	0.069 ± 0.003	0.0164 ± 0.0007
	9.4 ± 0.3	0.065 ± 0.003	0.0167 ± 0.0003
	27 ± 1	0.068 ± 0.007	0.0132 ± 0.0008

8.0	0.61 ± 0.04	0.0730 ± 0.0004	0.0289 ± 0.0004
	1.17 ± 0.03	0.078 ± 0.003	0.0282 ± 0.0010
	2.3 ± 0.1	0.076 ± 0.001	0.0283 ± 0.0006
	4.9 ± 0.1	0.081 ± 0.002	0.0284 ± 0.0004
	9.9 ± 0.3	0.079 ± 0.001	0.0275 ± 0.0010
	20.9 ± 0.6	0.086 ± 0.005	0.0277 ± 0.0004
8.5	0.57 ± 0.03	0.074 ± 0.001	0.0286 ± 0.0003
	0.92 ± 0.11	0.074 ± 0.002	0.0275 ± 0.0008
	1.6 ± 0.1	0.077 ± 0.004	0.0276 ± 0.0007
	4.0 ± 0.1	0.077 ± 0.002	0.0267 ± 0.0006
	8.4 ± 0.3	0.078 ± 0.002	0.0261 ± 0.0006
	18.2 ± 0.5	0.088 ± 0.002	0.0238 ± 0.0007
9.0	0.53 ± 0.03	0.0760 ± 0.0003	0.038 ± 0.001
	1.07 ± 0.03	0.077 ± 0.001	0.037 ± 0.001
	2.4 ± 0.1	0.086 ± 0.001	0.038 ± 0.001
	5.1 ± 0.1	0.093 ± 0.003	0.036 ± 0.001
	10.0 ± 0.3	0.092 ± 0.006	0.035 ± 0.002
	20.5 ± 0.5	0.10 ± 0.01	0.033 ± 0.002

Table S12. k_f and k_b, for the His73-heme alkaline conformational transition of AcH73 iso-1-Cyt*c* at 25 ^oC derived from fitting $k_{obs,2}$ data in Table S9 to eq 6 in the main text.

pH	k_b, s^{-1}	k_f, s^{-1}
5.0	29 ± 1	11.8 ± 3.4
5.5	25.5 ± 1.3	13.7 ± 5.5
6.0	22.9 ± 0.5	17.4 ± 2.5
6.5	18.7 ± 0.2	20.5 ± 1.1
7.0	15.2 ± 0.2	21.6 ± 1.8
7.5	14.1 ± 0.2	27.7 ± 1.5
8.0	13.0 ± 0.1	22.5 ± 1.3
8.5	12.5 ± 0.1	23.1 ± 1.3
9.0	12.0 ± 0.2	26.9 ± 1.8

Table S13. k_f and k_b, for AcH73 iso-1-Cyt*c* at 25 ^oC derived from fitting $k_{obs,3}$ data in Table S10 to eq 6 in the main text.

pH	k_b, s^{-1}	k_f, s^{-1}
5.0	3.0 ± 0.3	30 ± 16
5.5	3.5 ± 0.2	75 ± 19
6.0	2.8 ± 0.3	17 ± 14
6.5	2.5 ± 0.1	20 ± 6
7.0	2.7 ± 0.1	16 ± 5
7.5	2.5 ± 0.4	12 ± 14
8.0	0.8 ± 0.2	6 ± 20
8.5	0.41 ± 0.03	2 ± 6
9.0	0.45 ± 0.05	12 ± 9

Table S14. k_f and k_b, for AcH73 iso-1-Cyt*c* at 25 ^oC derived from fitting $k_{obs,4}$ data in Table S11 to eq 6 in the main text.

pH	k_b, s^{-1}	k_f, s^{-1}
5.0	0.066 ± 0.005	23 ± 11
5.5	0.060 ± 0.004	9 ± 8
6.0	0.062 ± 0.004	1 ± 5
6.5	0.067 ± 0.003	1 ± 3
7.0	0.059 ± 0.006	0 ± 9
7.5	0.070 ± 0.002	0 ± 1
8.0	0.082 ± 0.002	4 ± 2
8.5	0.082 ± 0.003	4 ± 2
9.0	0.096 ± 0.003	8 ± 2

D. Numerical Fitting of Gated ET Data

The steady-state approximation used to fit the k_{obs} versus a_6Ru^{2+} concentration data for the reduction of the His73-heme conformer of the AcH73 in Figure 8 of the main text (eq 6 in the main text, repeated here as eq S1) is only a good approximation when $k_{ET}[a_6Ru^{2+}] + k_f >> k_b$ (*1*).

$$k_{obs} = \frac{k_{ET} k_b [a_6 Ru^{2+}]}{k_{ET}[a_6 Ru^{2+}] + k_f} \quad \text{(S1)}$$

Thus, the steady-state approximation breaks down at low a_6Ru^{2+} concentration when $k_{ET}[a_6Ru^{2+}]$ approaches 100 s^{-1}. In Table S8, $k_{obs,1} = k_{ET}[a_6Ru^{2+}]$ approaches 100 s^{-1} for concentrations of $a_6Ru^{2+} < 2$ mM. Thus, the breakdown in the steady-state approximation is most prominent in a range of concentration critical for evaluating k_f with eq S1. Deviations from steady state-behavior are expected to be largest at low pH where k_b is largest and k_f is smallest.

The improved steady-state approximation which accounts for the fact that the concentration of the intermediate (Met80-heme conformer or native state of iso-1-Cyt*c* in our system) is not truly independent of time. For our system the improved state approximation yields eq S2 (*1*). In

$$k_{obs} = \frac{k_{ET} k_b [a_6 Ru^{2+}]}{k_{ET}[a_6 Ru^{2+}] + k_f + k_b} \quad \text{(S2)}$$

the low pH range, application of eq S2 to the data in Figure 8 of the main text yields physically unreasonable k_f values of negative magnitude. When $k_{ET}[a_6Ru^{2+}]$ approaches the magnitude of k_f and k_b, modeling results with the exact solution to the kinetic model involving a reversible equilibrium followed by an irreversible step show that both eqs S1 and S2 become poor approximations (*1*). Since $k_{obs,2}$ reported in Table S9 is expected to decrease faster than

predicted by the steady state approximation at low a_6Ru^{2+} concentration, the steady state approximation will tend to overestimate k_f (*1*). By contrast, since $k_{obs,2}$ is expected to decrease less rapidly than predicted by the improved steady-state approximation, the improved steady-state approximation will tend to underestimate k_f. It is worth noting that the exact expression for the kinetic model involving a reversible equilibrium followed by an irreversible step was derived assuming all species are at zero concentration except the species on the left of the reversible step (His73-heme conformer in our case). This assumption in not fulfilled by our system because all species are present at finite concentrations at the start of the reduction reaction. Thus, we have used numerical fitting of data near 1 mM a_6Ru^{2+}, where the steady-state approximation has clearly broken down to estimate k_f for the formation of the His73-heme conformer from the Met80-heme conformer of the AcH73 variant of iso-1-Cyt*c*.

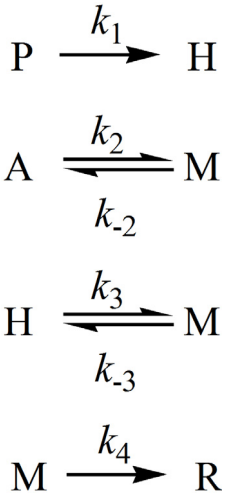

Scheme 1. Kinetic model used from pH 5 to 6.5.

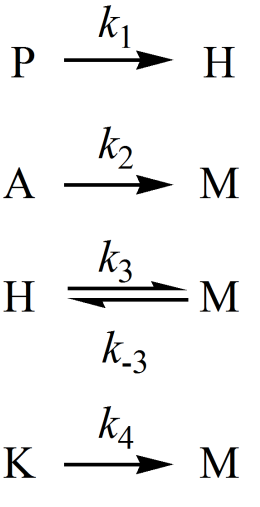

Scheme 2. Kinetic model used from pH 7 to 9.

Numerical fitting was carried out using Pro-Kineticist software, version 1 (Applied Photophysics, Inc.). Five separate data trials were fit at each pH using data acquired over a 50 s time scale. Thus, all four phases were included in the fit. Rate constants obtained from these fits are reported as the average and standard deviation of the five fits at each pH. Two different kinetic models are used as outlined in Schemes S1 and S2, where P is the His73-heme conformer with a cis-proline, H is the His73-heme conformer with the native trans-proline, A is an acid conformer in the low pH regime and an undefined conformer above pH

6.5, K is the Lys79-heme alkaline conformer, M is the native oxidized Met80-heme conformer and R is the reduced Met 80-heme conformer.

The following rate constant constraints were used in numerical fitting. The magnitude of k_1 was set equal to the limiting value of $k_{obs,4}$ (see Figure S12) obtained at high a_6Ru^{2+} concentration (Table S14). Above pH 7, k_1 was constrained to 0.06 since $k_{obs,4}$ begins to increase due to contributions from the reduction of the Lys79-heme conformer to this kinetic phase. k_4, the rate constant for conversion of the Lys79-heme conformer (K) to the Met80-heme conformer (M) in Scheme S2 was not constrained. The magnitude of k_2 was set equal to the limiting value of $k_{obs,3}$ (see Figure S11) obtained at high a_6Ru^{2+} concentration (Table S13). k_{-2} was not constrained at pH 5 to 6. At pH 6.5, k_{-2} produced values of zero within error and so it was set to zero in some fits. The magnitude of k_3 was set equal to the limiting value of $k_{obs,2}$ (see Figure 8, Main text) obtained at high a_6Ru^{2+} concentration (Table S12). k_{-3} was not constrained (this rate constant corresponds to $k_{f,num}$ in Figure 8 of the main text). The electron transfer rate constant (k_4 below pH 7 and k_5 pH 7 and above) was not constrained.

Rate constants from numerical fitting are sensitive to starting concentrations of species used in the model. To obtain total concentration we divided the amplitude at the lowest a_6Ru^{2+} concentration by the difference in the reduced versus oxidized extinction coefficient at 550 nm (19,000 $M^{-1}cm^{-1}$, *ref. 2*). Electron transfer is slow under these conditions and thus the entire amplitude is observed. The amplitude for each phase of the ~5 mM a_6Ru^{2+} trial (~5 mM was chosen because steady-state conditions apply and amplitudes reflect starting concentrations of species in solution) was divided by the total amplitude at the lowest a_6Ru^{2+} concentration. The resulting fractional amplitude was multiplied by the total concentration to produce starting concentrations from P, H, A and M, with the assumption that any decrease in total amplitude for

the ~ 5 mM a_6Ru^{2+} data relative to the lowest a_6Ru^{2+} concentration data was due to rapid reduction of M. At pH 7 and above, the ratio of P/H was assumed to remain constant with the remaining amplitude of the slowest phase being attributed to K. The extinction coefficient at 550 nm for M was constrained to 9000 M^{-1} cm^{-1}, the known extinction coefficient for oxidized cytochrome *c* at this wavelength (*2*). The extinction coefficient for P (His73-heme with a cis-proline) was constrained to 9000 M^{-1} cm^{-1} for fits to the mechanism in Scheme 2 because it took on negative values when unconstrained. Within error, this additional constraint did not affect rate constants obtained from numerical fitting. The fitted value for the extinction coefficient for R at 550 nm was always near 28,000 M^{-1} cm^{-1}, the known extinction coefficient for reduced cytochrome *c* at 550 nm (*2*). The rate constants obtained from numerical fitting are provided in Tables S15 and S16. Values from fits assuming a steady state approximation are included in Tables S15 and S16 for comparison. Representative fits to the data along with concentration profiles are shown in Figures S13 and S14.

Table S15. Rate constants from numerical fitting of gated ET data at ~1 mM a_6Ru^{2+} concentration for reduction of the AcH73 variant of iso-1-Cyt*c* at pH 5 to 6.5.

pH	$[a_6Ru^{2+}]$ mM	k_{-2}		k_{-3}		k_4	
		Numerical	Steady state[a]	Numerical	Steady state[b]	Numerical	Exponential fitting[c]
5.0	1.1 ± 0.1	20 ± 3	30 ± 16	6.4 ± 0.6	11.8 ± 3.4	74 ± 4	102 ± 2
5.5	1.1 ± 0.1	42 ± 1	75 ± 19	5.9 ± 0.6	13.7 ± 5.5	54 ± 2	102 ± 2
6.0	1.1 ± 0.1	10 ± 8	17 ± 14	13.8 ± 0.8	17.4 ± 2.5	73 ±8	99 ± 7
6.5	1.02 ±0.03	~0	20 ± 6	20.4 ± 0.4	20.5 ± 1.1	88 ± 1	113 ± 3

[a] k_f values from Table S13.

[b] k_f values from Table S12.

[c] $k_{obs,1}$ values at ~1 mM from Table S8.

From pH 5 to 6.5, the rate constant for the formation of the His73-heme conformer from the native state (Met80-heme conformer, k_{-3} in Table S15) from numerical fitting is lower than the values obtained from the steady state approximation. This result is expected based on the direction of deviation in $k_{obs,2}$ from the value expected for the steady state approximation. The intermediate (M, Met80-heme conformer) is highly populated at low pH, thus the deviation from steady-state behavior is expected to be largest. As expected, the electron transfer rate constant (k_4 in Table S15) is less than observed from directly fitting the exponential decay of the fast phase (*1*).

Table S16. Rate constants from numerical fitting of gated ET data at ~1 mM a_6Ru^{2+} concentration for reduction of the AcH73 variant of iso-1-Cyt*c* at pH 7 to 9.

pH	$[a_6Ru^{2+}]$ mM	k_{-3}		k_4		k_5	
		Numerical	Steady state[a]	Numerical	Steady state[b]	Numerical	Exponential fitting
7.0	1.30 ± 0.04	17.1 ± 1.0	21.6 ± 1.8	0.078 ± 0.002	0.059 ± 0.006	112 ± 2	113 ± 3
7.5	0.77 ± 0.06	28.5 ± 1.9	27.7 ± 1.5	0.089 ± 0.001	0.070 ± 0.002	65 ± 4	68 ± 8
8.0	1.17 ±0.03	31.4 ± 2.5	22.5 ± 1.3	0.084 ±0.002	0.082 ± 0.002	104 ± 7	106 ± 5
8.5	0.9 ± 0.1	23.9 ± 1.0	23.1 ± 1.3	0.081 ±0.001	0.082 ± 0.002	64 ±2	96 ± 10
9.5	1.07 ± 0.03	22.8 ± 3.2	26.9 ± 1.8	0.085 ±0.001	0.096 ± 0.003	46 ± 3	80 ± 12

[a] k_f values from Table S12.

[b] k_b values from Table S14.

[c] $k_{obs,1}$ values at ~1 mM from Table S8.

From pH 7 to 9, where the intermediate (M, Met80-heme) is poorly populated, the agreement of the rate constant for formation of the His73-heme conformer from the native state (Met80-

heme conformer, k_{-3} in Table S16) obtained from the steady-state approximation and from numerical methods is better.

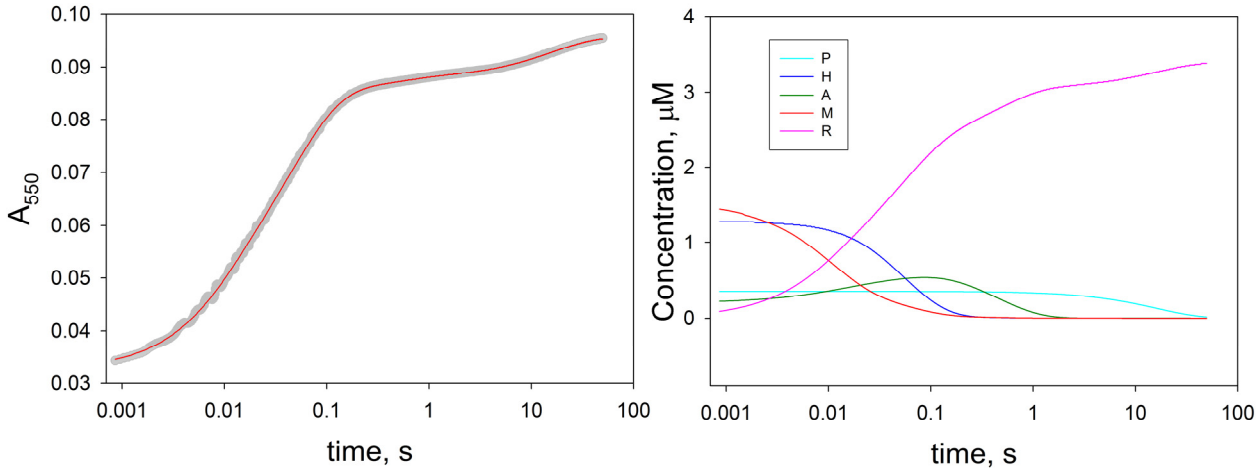

Figure S13. Numerical fit to data at pH 6 for reduction of the AcH73 variant of iso-1-Cyt*c* by 1 mM a_6Ru^{2+}. Left panel shows absorbance at 550 nm, A_{550}, versus time with data shown as gray circles and the fit as a red line. Right panel is the time dependent concentrations of the species in Scheme S1 obtained from the fit. The time axis in both panels is plotted logarithmically.

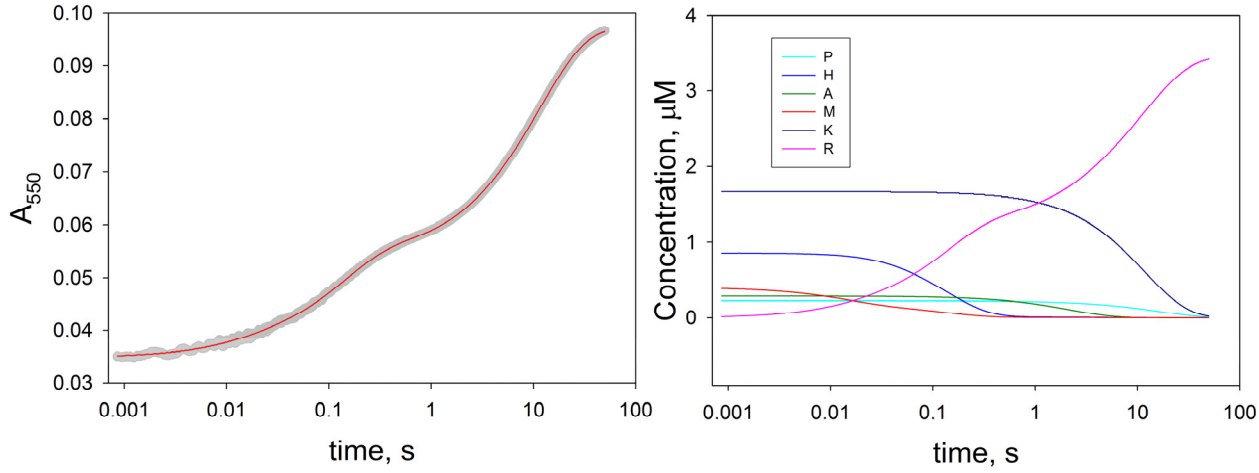

Figure S14. Numerical fit to data at pH 9 for reduction of the AcH73 variant of iso-1-Cyt*c* by 1.07 mM a_6Ru^{2+}. Left panel shows absorbance at 550 nm, A_{550}, versus time with data shown as gray circles and the fit as a red line. Right panel is the time dependent concentrations of the species in Scheme S2 obtained from the fit. The time axis in both panels is plotted logarithmically.

References

1. Espenson, J. H. (1995) *Chemical Kinetics and Reaction Mechanisms*, 2nd edition, pp. 77-90, McGraw-Hill, New York.
2. Margoliash, E., and Frohwirt, N. (1959) Spectrum of horse-heart cytochrome *c*, *Biochem. J. 71*, 570-572.